ACS APPLIED MATERIALS & INTERFACES

Research Article

www.acsami.org

Flexible Viologen Electrochromic Devices with Low Operational Voltages Using Reduced Graphene Oxide Electrodes

Jesús Palenzuela, Ana Viñuales, Ibon Odriozola, Germán Cabañero, Hans J. Grande, and Virginia Ruiz*

CIDETEC-IK4, Paseo Miramón 196, E-20009 Donostia-San Sebastian, Spain

ABSTRACT: Reduced graphene oxide (RGO) films have been electrodeposited on indium tin oxide-coated polyethylene terephthalate (ITO-PET) substrates from graphene oxide (GO) solutions, and the resulting flexible transparent electrodes have been used in electrochromic devices of ethyl viologen (EtV^{2+}). The electrochromic performance of devices with bare ITO-PET electrodes and ITO-PET coated with RGO has been compared. Under continuous cycling tests up to large voltages, the RGO film was oxidized and dispersed in the electrochromic mixture. The resulting devices, which contained GO and RGO in the electrochromic mixture, showed lower switching voltages between the colored and bleached states. This electrocatalytic activity of the solution-phase GO/RGO pair toward the electrochemical reaction of the electrochromic redox couple (the dication EtV^{2+} and the radical cation $EtV^{+\bullet}$) allowed devices with an optical contrast higher than the contrast of those free of GO at the same applied voltage.

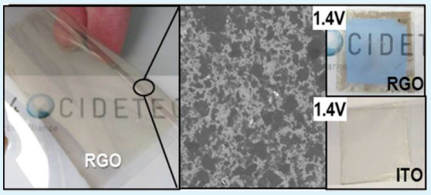

KEYWORDS: *electrochromism, flexible electrodes, graphene oxide, viologen*

1. INTRODUCTION

Electrochromism is defined as a reversible change in the transmittance of a material as the result of an electrochemical oxidation or reduction.[1] The electroactive species undergo changes in their optical absorption bands caused by the gain or loss of electrons. Commercial interest in electrochromism is mainly focused on smart windows, mirrors, and displays. In the simplest electrochromic devices, the electrochromic active molecules are dissolved in a medium interposed, as a single thin film, between the conductive inner surfaces of two transparent substrates. Among electrochromic materials, 1,1′-disubstituted 4,4′-bipyridinium salts (viologens) make up a well-known class of cathodic electrochromic compounds displaying different colors depending on their oxidation state and the nature of the substituents at the nitrogen atoms.[2] Thus, with simple alkyl groups, the dication species are colorless while the radical cations are blue/violet. The neutral, direduced compounds, formed by one-electron reduction of the radical cations or by direct two-electron reduction of the dications, show a weak color intensity.

In electrochromic devices (ECD), transparent conducting oxides (TCOs) and in particular tin-doped indium oxide (ITO) are the most commonly used electrode materials. However, ITO has several drawbacks. Indium is becoming a scarce and expensive resource, and ITO exhibits serious technical limitations (deposition techniques are expensive, and ITO films are fragile and sensitive to corrosion and have a relatively high refraction index). For these reasons, alternatives to TCOs such as organic polymers and nanomaterials are being investigated. Among the organic polymers, poly(3,4-ethylenedioxythiophene) doped with poly(styrenesulfonate) (PEDOT:PSS) is the leader in transparent conducting polymers. Thin coatings of metals, such as gold, and films of single-walled carbon nanotubes have also emerged as an alternative to ITO, with comparable transparency in the visible region and higher transparency in the 2−5 μm infrared region. Absorptive/transmissive polymer-based ECD have been assembled using single-walled carbon nanotubes on glass as electrode substrates.[3]

In this regard, the high transparency, electrical conductivity, and chemical stability of graphene make it an ideal electrode material for ECD as well as for many other electronic and optoelectronic applications such as solar cells,[4] touch screens,[5] light-emitting diodes,[6] and photodetectors.[7] In the field of electrochromism, after the first report of a graphene-based liquid crystal ECD,[8] there have been a number of studies of the effect of graphene or reduced graphene oxide on the electrochromic properties of a wide range of materials.[7−18] These have comprised both organic and inorganic electrochromic materials such as polyaniline,[9,10] poly(3,4-ethylenedioxythiophene),[11] poly(3,4-ethylenedioxypyrrole),[12] polynorbornenes,[13] polyimide,[14] polyamide,[15] Prussian blue,[16] nickel oxide,[17] tungsten oxide,[18] and vanadium pentoxide.[19]

Most of these studies focus on the preparation and evaluation of the electrochromic performance of novel graphene/electrochromic material composite films in a three-electrode cell configuration. Overall, there have been claims that the composite assemblies show good electrochromic features such as fast color-switching speed, good cyclic stability, and high coloration efficiency. However, only in a few cases has the performance of the hybrid system been benchmarked against the graphene-free counterpart. This is the case in ref 9, in which Zhao et al. demonstrated that polyaniline (PANI) on graphene-coated quartz electrodes showed much a greater

Received: June 17, 2014
Accepted: August 4, 2014
Published: August 4, 2014

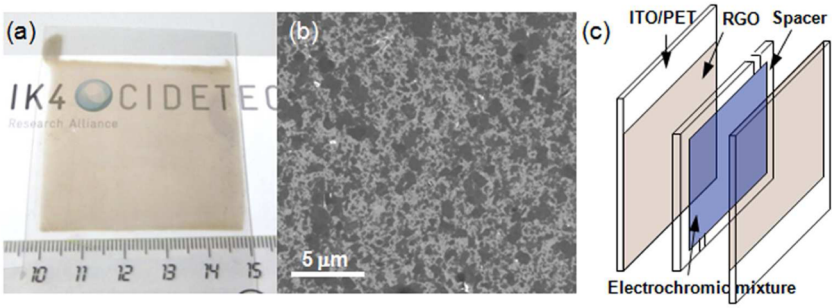

Figure 1. (a) Photograph of a RGO film electrodeposited on ITO-PET and (b) corresponding FESEM image showing the individual RGO sheets. (c) Schematic of the ECD assembly with the EtV^{2+}-containing electrochromic mixture sandwiched between two RGO-coated ITO-PET electrodes.

Scheme 1. Electrochemical Reactions Responsible for Color Changes in EtV^{2+}-Based ECD

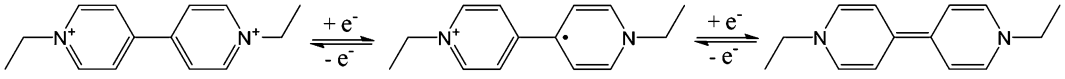

(EtV^{2+}) *Colorless* $(EtV^{+\cdot})$ *Colored* (EtV^{0}) *Weak color*

optical contrast and shorter switching time compared to those of PANI/ITO electrodes after 300 cycles, revealing the high electrochemical stability of graphene electrodes. Better cycling performance and faster switching speeds were also noted for NiO/RGO hybrid electrochromic films, which were attributed to the electrochemical stability of RGO and higher porosity of the hybrid film that facilitates electrolyte access.[17]

On the other hand, examples of fully assembled electrochromic devices integrating electrodes with graphene/electrochromic composite systems are scarce. In this paper, we report for the first time the preparation and spectroelectrochemical characterization of flexible ECD based on ethyl viologen (EtV^{2+}) sandwiched between two ITO-PET electrodes coated with RGO films. For the purpose of comparison, identical devices without the RGO coating (only ITO-PET) were also fabricated, and their electrochromic performance was assessed. Partial dissolution of the RGO film into the solution phase during potential cycling facilitated the redox reaction of the electrochromic system, which allowed a lower switching voltage between the colored and bleached states and consequently greater optical contrasts at a same applied voltage for the ECD fabricated with RGO electrodes.

2. EXPERIMENTAL SECTION

2.1. Materials. 1,1′-Diethyl-4,4′-bipyridinium dibromide (99%) was purchased from Aldrich and used without further purification. Hydroquinone (99.5%) was obtained from Riedel-de-Haën, and 1-butyl-3-methylimidazolium tetrafluoroborate (99%) was supplied by Solvionic. Extra pure propylene carbonate was purchased from Scharlau, and ITO-coated PET slides (R = 60 Ω/sq) were provided by Sheldahl.

2.2. Preparation of RGO-Coated ITO-PET Electrodes. Graphene oxide was produced by chemical exfoliation of natural graphite (Bay Carbon Inc., SP-1) according to the modified Hummers method.[20] Briefly, graphite was oxidized to graphite oxide in a H_2SO_4/$KMnO_4$/H_2O_2 mixture and subsequently exfoliated to graphene oxide by tip ultrasonication (3 h, ice bath) in an aqueous solution. Unexfoliated graphite oxide was separated by centrifugation (90 min, 4000 rpm), and the resulting stable aqueous graphene oxide (GO) dispersion was used to coat the ITO-PET electrodes. The GO aqueous solution (0.1 mg mL^{-1}) was placed between two ITO-PET substrates (5 cm × 5 cm) separated by 2 mm thick spacers with the two conducting surfaces facing each other. The potential difference between the two electrodes was gradually increased until a visible film of reduced graphene oxide was deposited at the cathode side. The RGO films on ITO-PET used in the ECD were deposited by applying a 3.5 V voltage for 5 min, which led to very homogeneous deposits of ~80%T at 550 nm.

2.3. Fabrication of the Electrochromic Device. The electrochromic mixture was prepared by mixing 1,1′-diethyl-4,4′-bipyridinium dibromide (0.01 g, 9 mM), hydroquinone (0.003 g, 9 mM), 1-butyl-3-methylimidazolium tetrafluoroborate ($BMIBF_4$, 1.6 g, 2 M), and propylene carbonate (2 g) for 1 h at room temperature. The ECD was prepared by joining two identical electrodes (either bare or RGO-coated ITO-PET) with an adhesive tape (200 μm thick) placed along the whole perimeter, allowing two small channels in opposite corners to fill the device by capillarity with the electrochromic mixture.

2.4. Instrumentation and Measurements. UV−vis absorption spectra were measured in transmission mode in a Jasco V-570 spectrophotometer. Transmittance of the ECD was registered using a film holder accessory for solid samples. All electrochemical measurements were taken with a Biologic MPG potentiostat-galvanostat. Cyclic voltammetry of deaerated EtV^{2+} solutions with an increasing concentration of GO was conducted in a three-electrode configuration with Pt foils as the working and counter electrode and a Ag wire as the pseudoreference electrode.

RGO films on ITO-PET were examined with a Carl Zeiss Ultra Plus field emission scanning electron microscope (FESEM) equipped with an energy dispersive X-ray spectrometer.

3. RESULTS AND DISCUSSION

Electrodeposition of RGO films on ITO-PET electrodes from GO aqueous solutions resulted in very homogeneous coatings at a relatively large scale, as illustrated in Figure 1a, where a 5 cm × 5 cm RGO deposit on an ITO-PET electrode is presented. A FESEM image of the RGO film (Figure 1b) shows the individual RGO sheets, which have a broad size distribution, with lateral dimensions ranging from hundreds of nanometers to several micrometers. Despite the apparent film heterogeneity at the nanoscale, the RGO deposit is macroscopically uniform as given by the film transmittance in different regions (80 ± 1%T at 550 nm). To test the performance of the RGO-coated ITO-PET electrodes in ECD, several viologen-based devices were fabricated using both uncoated and RGO-coated ITO-PET electrodes according to the schematic diagram depicted in Figure 1c. All the tested

devices were built with RGO-coated ITO-PET electrodes with the same transmittance to ensure the same amount of RGO. The electrochromic mixture containing EtV^{2+}, ionic liquid $BMIBF_4$ (as the electrolyte), and hydroquinone (as the redox mediator) dispersed in propylene carbonate was sandwiched between two identical ITO-PET (bare or RGO-coated) electrodes separated by a spacer. The typical size of the electroactive area was 2.5 cm × 2.5 cm.

Color changes in viologen-based ECD are due to the first electrochemical reaction in Scheme 1. The dicationic form (EtV^{2+}) of the first redox pair is colorless, whereas the reduced radical cation ($EtV^{+\bullet}$) is dark blue. The reversible change in color from colorless to blue was observed in all the devices when a voltage difference of ≥2 V was applied between the two ITO electrodes as a result of EtV^{2+} reduction at the cathode. Hereafter, we will refer to the potential difference (in absolute values) applied between the two electrodes as the operational voltage of the devices.

The UV−vis spectroelectrochemical response of identical EtV^{2+} ECD with bare and RGO-coated ITO-PET electrodes was investigated. Our initial aim was to probe whether the RGO film could act as an electrochemically stable protective barrier of ITO to enhance the ECD cycling stability, as previously reported for polyaniline films on RGO-coated quartz. Initially, ECD fabricated with both types of electrodes, bare and RGO-coated ITO-PET, exhibited very similar electrochromic performance in terms of optical contrast and switching response. Both ECD reached transmittance changes (Δ%T) of ∼55% at an applied voltage of 2 V in <20 s. However, in the course of continuous voltage cycling tests between 0 and 2 V, it was noted that RGO films were gradually depleted from the ITO surface. Photographs of a typical ECD after depletion of the RGO coating are displayed in panels a and b of Figure 2 in the bleached and colored states, respectively. It can be seen that a frame of an RGO film under the adhesive spacer remains, whereas in the area exposed to the electrochromic mixture, the film has come off.

This undesirable oxidative dissolution of RGO nonetheless caused a very interesting effect. In ECD, where RGO depletion occurred, and hence the GO/RGO redox pair (depending on the applied voltage) was incorporated into the electrochromic mixture, greater optical contrasts were achieved at a given voltage than in RGO-free ECD. The electrochromic response of ECD fabricated with bare and RGO-coated ITO-PET electrodes after RGO depletion is compared in panels c and d of Figure 2, where current density and transmittance changes at 600 nm (wavelength of maximal contrast for the $EtV^{2+}/EtV^{+\bullet}$ electrochromic pair) are plotted versus time during two consecutive potential steps between 1.5 and 0.0 V. The current density during the coloration (1.5 V) and bleaching (0.0 V) steps was higher for the ECD containing the GO/RGO redox pair in the solution phase. Differences in the optical contrast of both devices were even more remarkable, with Δ%T at 600 nm of 27% and only 3% for the ECD with and without the GO/RGO redox pair, respectively. Although at this voltage the switching speed is faster for the RGO-free ECD, this is due to its lower optical contrast. At voltages sufficiently high to drive the same transmittance changes in RGO-free ECD, the switching times are comparable.

The different response of the two types of ECD at increasing applied voltages is illustrated in the sequence of photographs shown in Figure 3. Color switching was achieved at significantly lower applied voltages in the device with the GO/RGO redox pair in the solution phase resulting from surface RGO depletion. While the ECD with bare ITO-PET electrodes did not show noticeable color changes below 1.5 V, the device fabricated with RGO-coated ITO-PET electrodes already

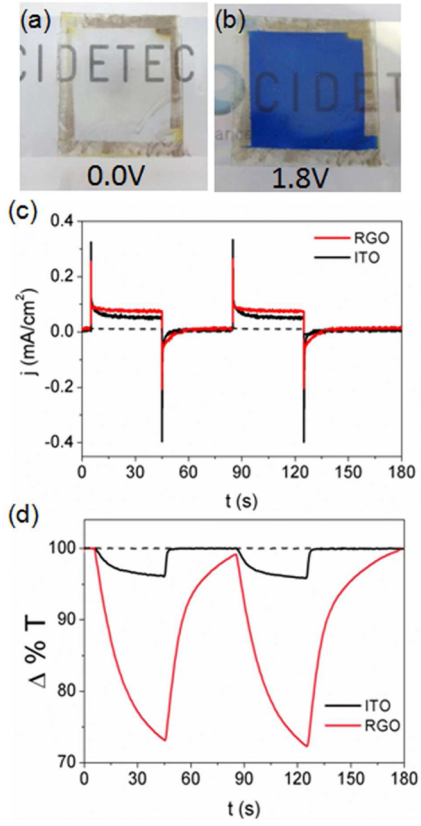

Figure 2. Photographs of an EtV^{2+} ECD after depletion of the RGO film from the ITO surface in the bleached (a) and colored state (b). Current density (c) and transmittance changes at 600 nm (d) measured during chronoamperometric potential steps between 1.5 and 0.0 V for EtV^{2+} ECD fabricated with bare (black) and RGO-coated (red) ITO-PET electrodes. Response of a device with RGO-coated ITO-PET electrodes and no EtV^{2+} present (---).

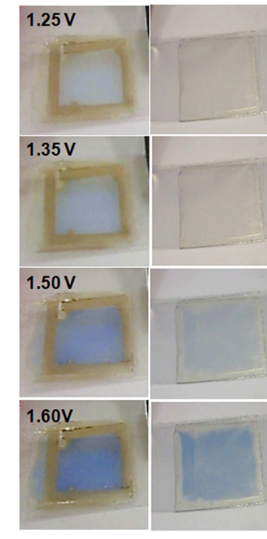

Figure 3. Photographs of EtV^{2+} ECD with the same composition fabricated with RGO-coated ITO-PET (left) and bare ITO-PET (right) electrodes at the applied voltages indicated in the figure.

switched to a perceptible pale blue color (Δ%T = 12%) at voltages as low as 1.25 V. This lower switching voltage was consistently found in several ECD (n > 4) fabricated with RGO-coated ITO-PET electrodes after the induction of an accelerated oxidative dissolution of RGO (applying >2.5 V for typically 2−3 min). However, when the applied voltage is gradually increased above a threshold value (1.7 V), both types of ECD start to show similar optical contrasts.

The voltage dependence of the optical contrast of ECD with and without the GO/RGO redox pair is highlighted in Figure 4.

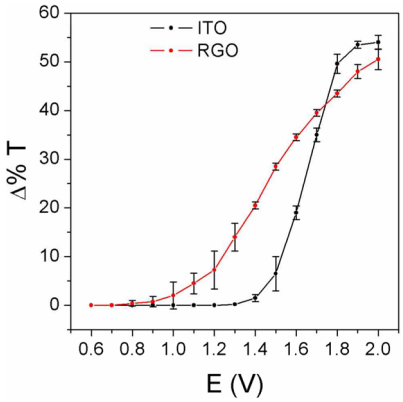

Figure 4. Transmittance changes at 600 nm at different applied voltages for several EtV^{2+} ECD fabricated with bare (black) and RGO-coated ITO-PET (red) electrodes. Transmittance values were taken at the end of each 30 s switching step between 0 V and the indicated voltages.

Changes in percent transmittance (Δ%T) for each type of device correspond to the difference between the %T measured at 600 nm at the end of each 30 s duration voltage step between 0 ($\%T_b$) and the different applied voltages ($\%T_c$). Figure 4 shows average Δ%T values from three ECD of each type, and the relative standard deviation is given by the corresponding error bars. It can be seen that an ECD with dispersed GO/RGO starts displaying measurable color switching at voltages as low as 1.0 V, whereas RGO-free devices require a voltage of 1.4 V to exhibit a comparable Δ%T (3−5%). That is, the transmittance−voltage curve of GO/RGO-containing ECD is shifted to lower voltages by 300−400 mV in the range of 1.0−1.5 V, which results in much greater optical contrasts at the same applied voltage for ECD fabricated with RGO-coated electrodes. At higher applied voltages, the difference in the response of both types of ECD starts to decrease, leveling off at 2.0 V.

It is known that the GO/RGO redox couple exhibits an electrochromic response.[21] Therefore, to rule out a possible contribution from the intrinsic electro-optical properties of GO/RGO to the electrochromic response of the ECD, we conducted spectroelectrochemical measurements of GO/RGO-containing ECD without the EtV^{2+} electrochrome. Because zero transmittance changes were measured in the voltage range of 0.6−2.0 V (Figure 2d), the greater optical contrast of GO/RGO-containing EtV^{2+} ECD cannot be explained by the contribution from GO/RGO electrochromism. Instead, the color switching at lower voltages indicates that the dispersed GO/RGO redox couple seems to be acting as a redox mediator of the electron transfer reaction of the $EtV^{2+}/EtV^{+\bullet}$ electrochromic pair.

To corroborate the GO/RGO-facilitated electrochemistry of the $EtV^{2+}/EtV^{+\bullet}$ pair, the effect of GO concentration in the cyclic voltammetry of EtV^{2+} solutions was examined using a three-electrode electrochemical cell. Figure 5 shows cyclic

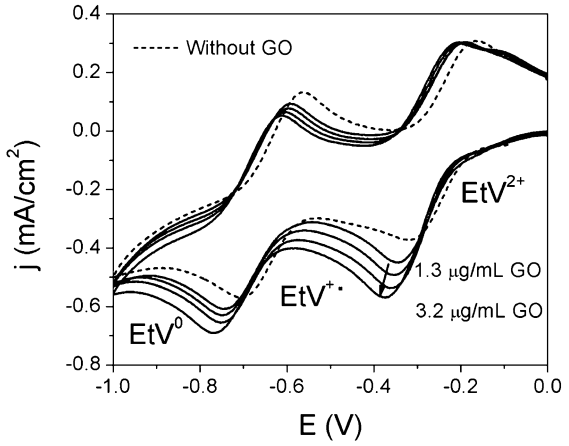

Figure 5. CV of 9 mM EtV^{2+} at a Pt electrode in a polycarbonate solution containing 2 M $BMIBF_4$ and 9 mM HQ at a scan rate of 50 mV s^{-1} (---). Solid lines show CV recorded in the presence of 1.3, 1.9, 2.6, and 3.2 μg mL^{-1} GO (the concentration increasing in the direction indicated by the arrow).

voltammograms (CV) of 9 mM EtV^{2+} at a Pt electrode in the same electrolyte solution as in the ECD in the presence of increasing GO concentrations. All CV exhibit the two pairs of reversible redox peaks corresponding to $EtV^{2+}/EtV^{+\bullet}$ and $EtV^{+\bullet}/EtV^{0}$ electrochemical reactions. It can be seen that the redox peaks shift to more negative potentials upon addition of GO to the EtV^{2+} solution along with a significant increase in the current density of the reduction peaks. The CV reveal that upon reduction of EtV^{2+} in the presence of GO, the electrochemically generated $EtV^{+\bullet}$ radicals undergo electron transfer with GO. This charge transfer interaction results in the reduction of GO and storage of electrons that can be used to further reduce the surface-confined EtV^{2+} and, hence, the enhanced reduction current densities. Similar electron donation from viologen radicals to graphene[22] and GO[23,24] has been previously demonstrated as well as the use of the transferred electrons to reduce other species such as Ag^+ ions to produce Ag silver nanoparticles on RGO.[23,24] Overall, these superior electrocatalytic properties of RGO for the electrochemical reactions of a large number of inorganic and organic electroactive compounds are the base for the development of RGO-based biosensors.[25] To a lesser extent, smaller family members such as graphene quantum dots (GQD) are also known to facilitate oxidation or reduction of some species (Ag^+ and H_2O_2),[26] and because of their charge transfer properties, they have recently been proposed as alternatives to conventional electrolytes in ECD of GQD-methyl viologen nanocomposites.[27]

In summary, we have shown that solution-phase GO/RGO from oxidative dissolution of RGO-coated electrodes acts as an electron mediator facilitating the $EtV^{2+}/EtV^{+\bullet}$ redox reaction and consequent color switching, thus allowing ECD to have lower operational voltages.

dx.doi.org/10.1021/am503869b | ACS Appl. Mater. Interfaces 2014, 6, 14562−14567

4. CONCLUSIONS

Flexible EtV^{2+} ECD have been prepared using ITO-PET electrodes and ITO-PET coated with a RGO film electrodeposited from GO aqueous solutions. The electrochromic response of ECD with bare ITO-PET and RGO-coated ITO-PET electrodes has been examined in the search for higher cycling stability for the RGO-coated electrodes. Initially, both types of ECD exhibited comparable optical contrast and switching times. However, a gradual oxidative dissolution of the RGO film occurred in the course of continuous voltage cycling tests. As a result, the GO/RGO couple was incorporated into the electrochromic solution, leading to ECD in which color switching was achieved at applied voltages lower than those in the GO/RGO-free devices. This electron mediator property of the GO/RGO redox couple in the electrochemical reaction of the $EtV^{2+}/EtV^{+\bullet}$ electrochromic system allowed ECD to have greater optical contrasts at a certain applied voltage. A possible contribution from the intrinsic electrochromic response of the GO/RGO redox couple was ruled out. These findings can be inspiring in the design of other types of ECD with lower operational voltages, thus preventing undesired degradation or side reactions, by incorporation of graphenelike materials with electrocatalytic properties into the electrochromic layer.

AUTHOR INFORMATION

Corresponding Author

*Telephone: 34 943 309 022. E-mail: vruiz@cidetec.es.

Author Contributions

J.P. and A.V. contributed equally to this work.

Notes

The authors declare no competing financial interest.

ACKNOWLEDGMENTS

Financial support from the Spanish MICINN (V .R. Ramón y Cajal Program) and the Basque Government (Etortek Program, nanoIKER Project IE11-304) is gratefully acknowledged.

REFERENCES

(1) Monk, P. M. S.; Mortimer, R. J.; Rosseinsky, D. R. *Electrochromism: Fundamentals and Applications*; VCH: Weinheim, Germany, 1995.

(2) Monk, P. M. S. *The viologens: Physicochemical Properties, Synthesis and Applications of the Salts of 4,4′-Bipyridine*; John Wiley & Sons: New York, 1998.

(3) Vasilyeva, S. V.; Unur, E.; Walczak, R. M.; Donoghue, E. P.; Rinzler, A. G.; Reynolds, J. R. Color purity in polymer electrochromic window devices on indium-tin oxide and single-walled carbon nanotube electrodes. *ACS Appl. Mater. Interfaces* **2009**, *1*, 2288−2297.

(4) Wang, X.; Zhi, L.; Müllen, K. Transparent, conductive graphene electrodes for dye-sensitized solar cells. *Nano Lett.* **2008**, *8*, 323−327.

(5) Bae, S.; Kim, H.; Lee, Y.; Xu, X.; Park, J.-S.; Zheng, Y.; Balakrishnan, J.; Lei, T.; Kim, H. R.; Song, Y. I.; Kim, Y.-J.; Kim, K. S.; Özyilmaz, B.; Ahn, J.-H.; Hong, B. H.; Iijima, S. Roll-to-roll production of 30-in. graphene films for transparent electrodes. *Nat. Nanotechnol.* **2010**, *5*, 574−578.

(6) Wu, J.; Agrawal, M.; Becerril, H. A.; Bao, Z.; Liu, Z.; Chen, Y.; Peumans, P. Organic light-emitting diodes on solution-processed graphene transparent electrodes. *ACS Nano* **2010**, *4*, 43−48.

(7) Xia, F.; Mueller, T.; Lin, Y.-M.; Valdes-Garcia, A.; Avouris, P. Ultrafast graphene photodetector. *Nat. Nanotechnol.* **2009**, *4*, 839−843.

(8) Blake, P.; Brimicombe, P. D.; Nair, R. R.; Booth, T. J.; Jiang, D.; Schedin, F.; Ponomarenko, L. A.; Morozov, S. V.; Gleeson, H. F.; Hill, E. W.; Geim, A. K.; Novoselov, K. S. Graphene-based liquid crystal device. *Nano Lett.* **2008**, *8*, 1704−1708.

(9) Zhao, L.; Zhao, L.; Xu, Y.; Qiu, T.; Zhi, L.; Shi, G. Polyaniline electrochromic devices with transparent graphene electrodes. *Electrochim. Acta* **2009**, *55*, 491−497.

(10) Sheng, K.; Bai, H.; Sun, Y.; Li, C.; Shi, G. Layer-by-layer assembly of graphene/polyaniline multilayer films and their application for electrochromic devices. *Polymer* **2011**, *52*, 5567−5572.

(11) Saxena, A. P.; Deepa, M.; Joshi, A. G.; Bhandari, S.; Srivastava, A. K. Poly(3,4-ethylenedioxythiophene)-ionic liquid functionalized graphene/reduced graphene oxide nanostructures: Improved conduction and electrochromism. *ACS Appl. Mater. Interfaces* **2011**, *3*, 1115−1126.

(12) B. Reddy, N.; Deepa, M.; Joshi, A. G.; Srivastava, A. K. Poly(3,4-ethylenedioxypyrrole) enwrapped by reduced graphene oxide: How conduction behavior at nanolevel leads to increased electrochemical activity. *J. Phys. Chem. C* **2011**, *115*, 18354−18365.

(13) Lian, W.-R.; Huang, Y.-C.; Liao, Y.-A.; Wang, K.-L.; Li, L.-J.; Su, C.-Y.; Liaw, D.-J.; Lee, K.-R.; Lai, J.-Y. Flexible electrochromic devices based on optoelectronically active polynorbornene layer and ultratransparent graphene electrodes. *Macromolecules* **2011**, *44*, 9550−9555.

(14) Ma, L.; Niu, H.; Cai, J.; Zhao, P.; Wang, C.; Bai, X.; Lian, Y.; Wang, W. Photoelectrochemical and electrochromic properties of polyimide/graphene oxide composites. *Carbon* **2014**, *67*, 488−499.

(15) Ma, L.; Niu, H.; Cai, J.; Zhao, P.; Wang, C.; Lian, Y.; Bai, X.; Wang, W. Optical, electrochemical, photoelectrochemical and electrochromic properties of polyamide/graphene oxide with various feed ratios of polyamide to graphite oxide. *J. Mater. Chem. C* **2014**, *2*, 2272−2282.

(16) Ko, J. H.; Yeo, S.; Park, J. H.; Choi, J.; Noh, C.; Son, S. U. Graphene-based electrochromic systems: The case of prussian blue nanoparticles on transparent graphene film. *Chem. Commun.* **2012**, *48*, 3884−3886.

(17) Cai, G.-F.; Tu, J.-P.; Zhang, J.; Mai, Y.-J.; Lu, Y.; Gu, C.-D.; Wang, X.-L. An efficient route to a porous NiO/reduced graphene oxide hybrid film with highly improved electrochromic properties. *Nanoscale* **2012**, *4*, 5724−5730.

(18) Chang, X.; Sun, S.; Dong, L.; Hu, X.; Yin, Y. Tungsten oxide nanowires grown on graphene oxide sheets as high-performance electrochromic material. *Electrochim. Acta* **2014**, *129*, 40−46.

(19) Zhang, X.; Sun, H.; Li, Z.; Xu, J.; Jiang, S.; Zhu, Q.; Jin, A.; Zakharova, G. S. Synthesis and electrochromic characterization of vanadium pentoxide/graphene nanocomposite films. *J. Electrochem. Soc.* **2013**, *160*, H587−H590.

(20) Park, S.; An, J.; Piner, R. D.; Jung, I.; Yang, D.; Velamakanni, A.; Nguyen, S. T.; Ruoff, R. S. Aqueous suspension and characterization of chemically modified graphene sheets. *Chem. Mater.* **2008**, *20*, 6592−6594.

(21) Ekiz, O. O.; Ürel, M.; Güner, H.; Mizrak, A. K.; Dâna, A. Reversible electrical reduction and oxidation of graphene oxide. *ACS Nano* **2011**, *5*, 2475−2482.

(22) Jeong, H. K.; Kim, K.-J.; Kim, S. M.; Lee, Y. H. Modification of the electronic structures of graphene by viologen. *Chem. Phys. Lett.* **2010**, *498*, 168−171.

(23) Krishnamurthy, S.; Lightcap, I. V.; Kamat, P. V. Electron transfer between methyl viologen radicals and graphene oxide: Reduction, electron storage and discharge. *J. Photochem. Photobiol., A* **2011**, *221*, 214−219.

(24) Lightcap, I. V.; Kosel, T. H.; Kamat, P. V. Anchoring semiconductor and metal nanoparticles on a 2-dimensional catalyst mat. Storing and shuttling electrons with reduced graphene oxide. *Nano Lett.* **2010**, *4*, 577−583.

(25) Zhou, M.; Zhai, Y.; Dong, S. Electrochemical sensing and biosensing platform based on chemically reduced graphene oxide. *Anal. Chem.* **2009**, *81*, 5603−5613.

(26) Chen, S.; Hai, X.; Chen, X.-W.; Wang, J.-H. In-situ growth of silver nanoparticles on graphene quantum dots for ultra-sensitive

colorimetric detection of H_2O_2 and glucose. *Anal. Chem.* **2014**, *86*, 6689−6694.
(27) Hwang, E.; Seo, S.; Bak, S.; Lee, H.; Min, M.; Lee, H. An electrolyte-free flexible electrochromic device using electrostatically strong graphene quantum dot−viologen nanocomposites. *Adv. Mater.* **2014**, DOI: 10.1002/adma.201401201.